



# Preparation of low molecular weight *Enteromorpha prolifera* polysaccharide and its antioxidant and tyrosinase inhibitory activities

Fei QUE<sup>1\*</sup> , Ying WANG<sup>2</sup>, Liping WANG<sup>2</sup>, Lin ZHAO<sup>1</sup>, Hannian HUANG<sup>1</sup>

## Abstract

*Enteromorpha prolifera* polysaccharide (EP) is a water-soluble sulfated polysaccharide with many types of biological activities. In this study, the crude polysaccharide was extracted from *Enteromorpha prolifera* and degraded by different physical, chemical, and biological methods. The results showed that the enzymatic degradation products displayed the best tyrosinase inhibitory activity. The optimal enzymatic degradation conditions were as follows: 30 °C, pH 5.5, 750 U/mL enzyme dosage for 2 h. The enzymatic hydrolysates were then divided into six EP fractions (EPFs) by an ultrafiltration membrane. The *in vitro* tyrosinase inhibitory activity of these fractions showed that the smaller the molecular weight of EPF, the better the inhibitory effect on tyrosinase. The antioxidant and tyrosinase inhibitory effect of the most effective EPF, a molecular weight below 5 kDa, (EPF5), was further confirmed on B16 cells. A kinetic study of tyrosinase inhibitory activity revealed that EPF5 is a competitive-uncompetitive mixed-type inhibitor of tyrosinase. These findings suggested that EPF5 has significant potential as a skin-whitening agent in cosmetics as well as an antibrowning agent in the food and agriculture industries.

**Keywords:** *Enteromorpha prolifera* polysaccharide; enzymatic degradation; low molecular weight; tyrosinase inhibitory activity; antioxidant activity.

**Practical Application:** This study provides a basis for the industrial application of *Enteromorpha prolifera* polysaccharide.

## 1 Introduction

*Enteromorpha* (*Ulva*) *prolifera* is a multicellular eukaryote belonging to the phylum Chlorophyta and the family Ulvaceae (Liu et al., 2020). Green tides dominated by *Enteromorpha prolifera* are present in the Southern Yellow Sea, China, for 15 consecutive years. They not only damage the marine environment but also cause economic losses to coastal cities (Xia et al., 2022). However, *Enteromorpha prolifera* is also considered a marine bioresource. *Enteromorpha prolifera* polysaccharide (EP) constitutes the main component of the cell wall and accounts for nearly 18% of the dry weight. It possesses various physiological properties such as antioxidant, anticoagulant, antitumor, antiaging, immune regulatory activities, elimination of inflammation, anti-tumor activity in skin cancer, skin-protective activities, and so on (Cao et al., 2020; Ning et al., 2022). Thus, EP holds a promising potential in the food industry as a new functional food, or as an additive in the cosmetics industry for natural products-based cosmeceuticals (Arokiarajan et al., 2022; Fernando et al., 2019). The most important activity of EP is the antioxidant activity, which is closely related to the anti-aging, antitumor, and other properties of polysaccharides (Zhou et al., 2021). Because of the waste utilization, high content, and excellent bioactivities of EP, its extraction and investigation of the antioxidant activity add to the high-valued utilization of *Enteromorpha prolifera* (Wassie et al., 2021).

Tyrosinase (EC 1.14.18.1), also called polyphenol oxidase with an active center of Cu<sup>2+</sup>, is widely distributed in animals, plants, microorganisms, and insects and plays an important role in melanogenesis and enzymatic browning. It is the rate-limiting enzyme in the production of dopa from tyrosine and its subsequent oxidation to melanin (Goenka & Simon, 2021). Thus, it is associated with skin health and undesirable enzymatic browning of fruits and vegetables (Zhou et al., 2021). Therefore, the inhibitors of tyrosinase which can be considered antioxidants, are extensively used in cosmetics and medical industries as depigmenting agents and in food and agriculture industries as antibrowning agents (Zhang et al., 2021). Tyrosinase inhibitors developing for novel food preservatives have attracted the attention of more and more scholars. For example, Wang et al. (2021) reported that the fucoidan fraction with MW below 5 kDa demonstrated strong tyrosinase inhibitory effect and shown obvious browning inhibition of fresh-cut apple slices (Wang et al., 2021). Stilbene-hydroxypyridinone hybrid, gallic acid-benzylidenehydrazine hybrid, the synthetic tyrosinase inhibitors, exhibited capacity to preserve fresh-cut apples and shrimps (Zhu et al., 2022; Peng et al., 2022).

Sulfated polysaccharides, degraded low-molecular-weight polysaccharides, or oligosaccharides derived from seaweed have been reported to be effective as tyrosinase inhibitors. *Sargassum fusiforme* polysaccharides can inhibit both monophenolase and

Received 11 June, 2022

Accepted 22 Aug., 2022

<sup>1</sup> College of Applied Engineering, Zhejiang Institute of Economics and Trade – ZJIET, Hangzhou, Zhejiang, China

<sup>2</sup> College of Food Science and Engineering, Qingdao Agricultural University – QAU, Qingdao, China

\*Corresponding author: trophyquefei@sina.com

diphenolase activity of mushroom tyrosinase in a dose-dependent manner. The degraded polysaccharides have superior inhibitory activities than the original polysaccharides (Chen et al., 2016). *Hizikia fusiforme* polysaccharides inhibit melanogenesis by down-regulating intracellular levels of tyrosinase and tyrosinase-related protein-1 and-2 via inhibition of microphthalmia-associated transcription factor expression (Wang et al., 2020). Sulfated galactans from red seaweed *Gracilaria fisheri* have been reported to significantly suppress cellular tyrosinase activity and melanin production in B16F10 melanoma cells without any obvious cytotoxicity (Pratoomthai et al., 2018). The enzymatically degraded polysaccharides from *Enteromorpha prolifera* are found to have stronger tyrosinase inhibitory effects than the raw polysaccharides. The inhibition of the degraded polysaccharides on the diphenolase activity of mushroom tyrosinase is found to be reversible and of a competitive-uncompetitive mixed type (Zhou et al., 2021). Besides the studies mentioned above, the research on the anti-tyrosinase activity of EP is very limited.

It has been found that undegraded EPs have limited applications due to their large molecular weight, poor water solubility, and poor biocompatibility (Guo et al., 2019). Scholars have tried different methods to degrade EPs into low molecular weight polysaccharides or oligosaccharides (Yin et al., 2019). Different degradation methods have different efficiencies and pose different effects on product activities. Currently, EPs can be degraded via physical degradation, chemical degradation, and biological degradation methods. Physical degradation mainly includes radiation degradation, ultrasonic degradation, plasma degradation, etc. (Zhong et al., 2015). Chemical degradation mainly includes acid hydrolysis and free radical degradation (Gu et al., 2021). Among these methods, acid hydrolysis is a traditional method of polysaccharide degradation, which is simple and easy to use. The biodegradation process also includes enzymatic degradation. This degradation method has received considerable attention due to its advantages of environmental compatibility, high efficiency, and mild reaction conditions (Wang et al., 2021). In our previous work, the use of fucoidanase produced by Flavobacteriaceae RC2-3 (Chen et al., 2019) and Flavobacteriaceae RC2-3 Mut. (Wang et al., 2021) has been proven to increase the antioxidant activity of *Laminaria japonica* polysaccharides. The present work intended to compare and optimize the preparation methods of EP using the tyrosinase inhibition rate as an evaluation index and consequently prepared the degraded EP by *Flavobacterium* RC3 Mut. Then, the antioxidant and tyrosinase inhibitory activities of the degraded EP were verified through cell experiments, and the preliminary inhibition mechanism of its tyrosinase activity was explored through a kinetics study. Thus, the present work will lay the foundation for the better utilization of EP as a functional food, antibrowning agent, and in cosmetics and medicine.

## 2 Materials and methods

### 2.1 Reagents and materials

*Enteromorpha prolifera* was collected from Huiquan Bay, Qingdao. EP Enzyme was provided by the Functional Food Research and Development Laboratory of Qingdao Agricultural University. Arbutin, L-tyrosine, B16 mouse melanoma cell, and

mushroom tyrosinase were purchased from Sigma Chemical Co. (Shanghai, China). Q Sepharose Fast Flow (QFF) column was purchased from Beijing Solarbio Science & Technology Co., Ltd. (Beijing, China). All chemicals and reagents used in the study were of analytical grade.

### 2.2 Extraction of polysaccharides from *Enteromorpha prolifera*

The dried *Enteromorpha prolifera* was immersed in distilled water with a solid-to-liquid ratio of 1:40 (g/mL). The tissues were pulverized, heated (95 °C, 15 min), cooled, and then filtered. The filtrate was concentrated to a water content of 95% and centrifuged (8000 rpm, 10 min, 4 °C). The supernatant was collected and precipitated by adding 80% ethanol (24 h), followed by freeze-drying to obtain crude EP.

### 2.3 Purification of EP

The polysaccharide purification method was followed as described by Chen et al. (2019). Briefly, the crude EP was dissolved in distilled water to prepare an EP solution of 4 mg/mL. The solution was loaded on the QFF anion exchange column (2.6 × 30 cm), which was pre-equilibrated with distilled water. Elution was done with NaCl as the mobile phase and a gradient of 0, 1.0, 1.5, and 2.0 mol/L at a flow rate of 2 mL/min. Each concentration gradient of NaCl was used to elute a column volume, and one tube was collected at every 5 mL of the eluent. EP content was determined by the phenol sulfuric acid method. Briefly, 800 µL of phenol (5%) was added to 0.5 mL of the sample, followed by 3.5 mL of sulfuric acid (98%), and absorbance at 490 nm was measured. The fraction with the highest polysaccharide content and the best tyrosinase inhibition rate (EP3; according to the result shown in Figure 1) was used for the following degradation step. NaCl was removed by dialysis, and the purified EP3 was lyophilized for storage.

### 2.4 Degradation of polysaccharides

Physical degradation of EP3 was carried out by the ultrasonic degradation method with 1 mg/mL of EP3 and 200 W ultrasonic power for 15 min (Zhong et al., 2015).

Chemical degradation was carried out by the acid hydrolysis method. Briefly, EP3 was dissolved in water at 1 mg/mL and hydrolyzed with 0.1 mol/L sulfuric acid at 80 °C for 60 min (Gu et al., 2021).

Biodegradation was carried out by the enzymatic hydrolysis method. EP enzyme obtained according to previous study was used for the enzymatic hydrolysis of EP3 (750 U/mL of EP enzyme, pH 5.5, 30 °C, 2 h) (Wang et al., 2021). Briefly, Flavobacteriaceae RC3, the wild degrading strain, was screened from kelp and optimized to enhance the enzyme yield by UV irradiation. Degrading enzyme produced by mutagenized Flavobacteriaceae RC3 was purified following the method of Chen et al. (2019). The hydrolysate was separated into EP fractions (EPFs) by an ultrafiltration membrane.

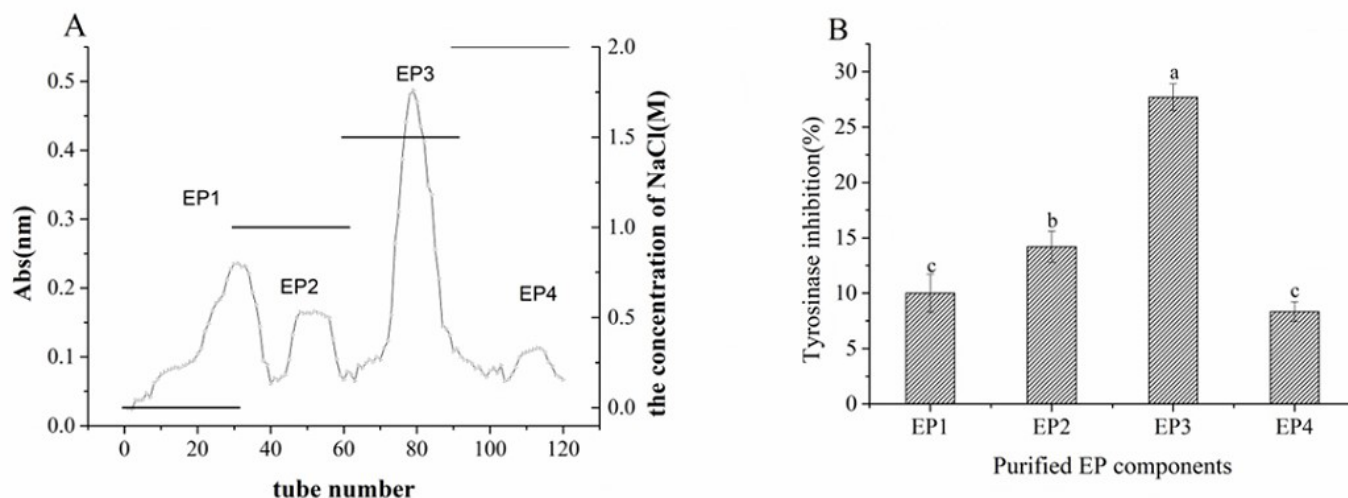


**Figure 1.** Separation and purification of EP using a QFF-anion exchange column (A) and determination of the tyrosinase inhibitory activity of each purified EP fraction (B). Values are expressed as mean  $\pm$  SD,  $n = 10$ . a, b, c,... means each parameter with different letters is significantly different at  $p < 0.05$ .

### 2.5 Determination of tyrosinase inhibition rate

The tyrosinase inhibition rate was determined according to the method described previously (Wang et al., 2021) with minor modifications. Briefly, a phosphate buffered solution of pH 6.8 was prepared by mixing sodium dihydrogen phosphate and disodium hydrogen phosphate solutions (separately prepared in distilled water). L-tyrosine was dissolved in hydrochloric acid, followed by the addition of phosphate buffer solution, and placed in an ice bath. Tyrosinase (5000 U) was dissolved in the phosphate solution and sub-packaged in an ice bath, followed by incubation at  $-20^{\circ}\text{C}$ . The formula for inhibition rate calculation is shown in Equation 1:

$$\text{Tyrosinase inhibition rate (\%)} = \frac{(A1 - A2) - (B1 - B2)}{A1 - A2} \times 100\% \quad (1)$$

### 2.6 Measurement of antioxidant activity

The antioxidant activity was measured by DPPH free radical scavenging assay using standard methods of evaluation (Molina et al., 2019). Briefly, 0.5 mL of the sample was dissolved in 1.1 mL of distilled water and mixed with 2.4 mL of DPPH (0.1 mM) in the sample test tube. DPPH was replaced with absolute ethanol in the reference tube. The control tube contained 2.4 mL of DPPH (0.1 mM) mixed with 1.6 mL of distilled water. The absorbance of each tube was measured at 519 nm. The formula used for the calculation of the DPPH radical scavenging rate is shown in Equation 2:

$$\text{DPPH radical scavenging rate (\%)} = \left( 1 - \frac{A_{\text{sample}} - A_{\text{reference}}}{A_{\text{control}}} \right) \times 100\% \quad (2)$$

### 2.7 Determination of cell viability

Cell proliferation was assessed by the MTT assay (Ou et al., 2014). When B16 cells reached 80% confluency, subculturing was done, and the ninth generation was selected to set up the

experiment, positive, and control group. After the cells completely adhered to the wall, the original medium was removed, and 100  $\mu\text{L}$  DMEM (high glucose, without phenol red) containing different concentrations of samples was added. Five concentration gradients (10, 5, 2.5, 1, and 0.5 mg/mL) of EP3, EPF5 (EPF with  $< 5$  kDa), and arbutin were set with six replicates per concentration gradient. The blank group was treated with the same amount of distilled water. After incubation in a 5%  $\text{CO}_2$  incubator at  $37^{\circ}\text{C}$  for 24 h, 200  $\mu\text{L}$  of 0.5 mg/mL MTT medium was added to each well and further incubated for 4 h. MTT-containing medium was then removed, and 200  $\mu\text{L}$  of dimethyl sulfoxide was added to each well. The plate was kept on an oscillator for 10 min and read at 490 nm by a microplate reader. The average value of six replicated wells was calculated to determine cell viability. Baseline cell viability in control wells not exposed to EP3, EPF5, and arbutin was set at 100%.

### 2.8 Determination of intracellular melanin content of B16 cells

B-16 cells were cultured to the logarithmic growth phase and detached from the culture flask by adding trypsin. Detached cells were resuspended in 2 mL complete DMEM for cell counting with a total of  $1 \times 10^5$  cells. The experimental group and the control group were set at a concentration of  $1 \times 10^3$  cells/well in a 96-well plate and incubated for 8-10 h. Then, the culture medium was removed after the cells adhered to the walls and added with a fresh medium containing different concentrations (25, 50, 100, 250, and 500  $\mu\text{g}/\text{mL}$ ) of EP3, EPF5, and arbutin with six replicates per concentration gradient. The plates were incubated for 72 h in a 5%  $\text{CO}_2$  incubator at  $37^{\circ}\text{C}$ . Then, the cells were washed in cold phosphate buffer (PBS) and incubated with 1 M NaOH (1 mL) and 10% dimethyl sulfoxide at  $80^{\circ}\text{C}$  for 1 h. Further, vortexing was done to dissolve melanin, and the absorbance was measured at 450 nm. Equation 3 was used for calculating melanin production inhibition rate:

$$\text{Melanin production inhibition rate (\%)} = \frac{\text{control group} - \text{experimental group}}{\text{control group}} \times 100\% \quad (3)$$

### 2.9 Determination of tyrosinase activity in B16 cells

B16 cells at a concentration of  $1 \times 10^4$  cells/well were cultured in a 12-well plate. After the cells completely adhered to the wall, the culture medium containing different concentrations of EP3, EPF5, and arbutin was added. The concentration gradients used were: 25, 50, 100, 250, and 500  $\mu\text{g/mL}$ ; six replicates of each concentration were set and cultured with different concentrations of polysaccharides for 72 h. Further, the cells were washed with PBS, 100  $\mu\text{L}$  sample was added to each well, frozen at  $80^\circ\text{C}$  for 30 min, thawed, and heated in a water bath at  $37^\circ\text{C}$  to accelerate the dissolution of the cells. Of 10  $\text{mg/mL}$  L-dopa, 100  $\mu\text{L}$  was added to each well, incubated at  $37^\circ\text{C}$  for 4 h, and the absorbance was measured by a microplate read at 490 nm. Each well was read 3 times, and the tyrosinase inhibition rate of different samples was calculated using the Equation 4:

$$\text{Tyrosinase inhibition rate (\%)} = \frac{\text{control group} - \text{experimental group}}{\text{control group}} \times 100\% \quad (4)$$

### 2.10 Determination of reactive oxygen species in B16 cells

The ninth generation of B16 cells in their logarithmic growth phase was taken, and the cell concentration was adjusted by using the complete medium. The cells were inoculated into 24-well plates at a density of  $1 \times 10^5$  cells/well (0.5 mL/well) and cultured in a 5%  $\text{CO}_2$  incubator at  $37^\circ\text{C}$ . At 90% confluency, the experiment was set as follows: ① Blank group: distilled water + UVB irradiation for 10 min; ② Positive group: 0.5  $\text{mg/mL}$  arbutin + UVB radiation for 10 min; ③ Control group: 0.5  $\text{mg/mL}$  EP3 + UVB radiation for 10 min; and ④ Experimental group: 0.5  $\text{mg/mL}$  EPF5 + UVB irradiation for 10 min. The culture medium was discarded, the cells were rinsed 3 times with PBS leaving a small amount of PBS in wells, and further cultured for 24 h in the new medium. After incubation, the medium was discarded, and the cells were again rinsed 3 times with PBS (3 min each time). The fluorescence intensity of rinsed cells was measured at the excitation wavelength of 500 nm and the emission wavelength of 525 nm, and cells were photographed under the fluorescence microscope for recording.

### 2.11 Kinetic inhibition of tyrosinase activity by EPF

The classification of EPF5 has already been described in 2.3 of the methods. The kinetics of tyrosinase inhibitory activity by EPF5 were analyzed using the Lineweaver-Burk Plot method. Tyrosinase at 500 U/mL concentration and 0.2, 0.4, 0.6, 0.8  $\text{mg/mL}$  of L-3,4-dihydroxyphenylalanine (L-DOPA, substrate) were used.

### 2.12 Statistical analysis

Parametric data were expressed as means  $\pm$  SD. Statistical comparisons among different groups were carried out using one-way ANOVA and Duncan's multiple range test.  $p < 0.05$  was considered statistically significant.

## 3 Results and discussion

### 3.1 Extraction and purification of EP

According to the elution capacity of different EP components, each concentration of NaCl washes out a separate component peak. As shown in Figure 1A, four fractions were named EP1, EP2, EP3, and EP4. The tyrosinase inhibitory activity of these four components was measured, and the results showed that EP3, which had the highest polysaccharide content (31.37%), possessed the strongest tyrosinase inhibitory activity (28.1%). The EP3 component was thus utilized for subsequent studies.

### 3.2 Comparison of three degradation methods

In this study, three degradation methods were used to degrade EP3 under optimal conditions. The degradation products of all three methods were compared with raw sugar (RS) for the tyrosinase inhibitory activity. As shown in Figure 2, the physical degradation products (PDP) showed 29.3% inhibitory activity, the chemical degradation products (CDP) showed 32.5%, and the enzymatic degradation products (EDP) showed 43.7% of the tyrosinase inhibitory activity. These results indicated that enzymatic hydrolysis had the best degradation effect. Therefore, the enzymatic degradation method was selected for subsequent experiments.

### 3.3 Tyrosinase inhibition activity of EPFs with different molecular weight (MW)

EP3 was separated by an ultrafiltration system to obtain 6 components with different molecular weights:  $> 100$  kDa, 50-100 kDa, 30-50 kDa, 10-30 kDa, 5-10 kDa, and  $< 5$  kDa. The in vitro tyrosinase inhibitory activity of each component was measured (Figure 3). EPF5 showed the highest tyrosinase inhibitory activity of 49.6%. According to Wang et al. (2021) when the enzymatically degraded fucoidan was graded through an

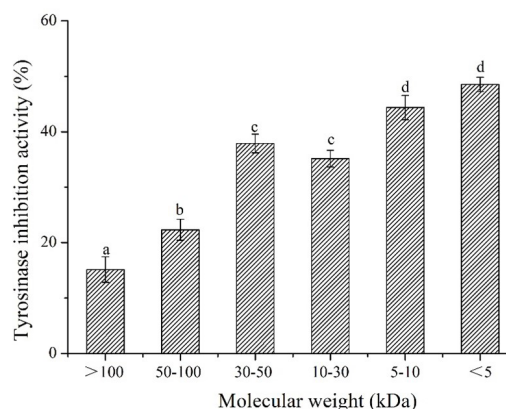


**Figure 2.** The tyrosinase inhibition rate of polysaccharides degraded by different methods. RS: raw sugar; PDP: physical degradation products; CDP: chemical degradation products; EDP: enzymatic degradation products. Values are expressed as mean  $\pm$  SD,  $n = 10$ . a, b, c,... means each parameter with different letters is significantly different at  $p < 0.05$ .

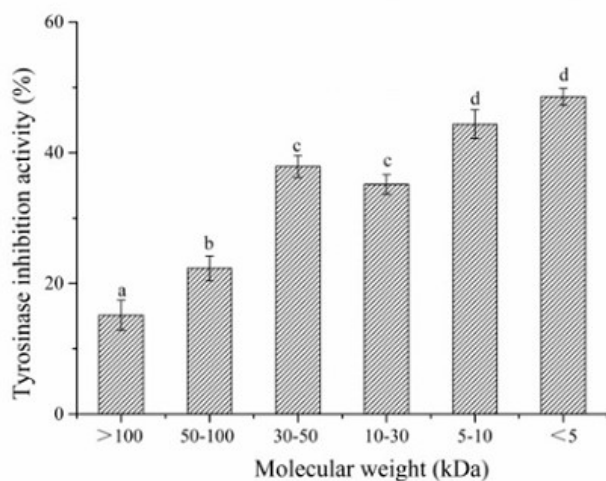


**Figure 3.** The tyrosinase inhibitory activity of *Enteromorpha prolifera* fractions with different molecular weights. Values are expressed as mean  $\pm$  SD, n = 10. a, b, c,... means each parameter with different letters is significantly different at  $p < 0.05$ .

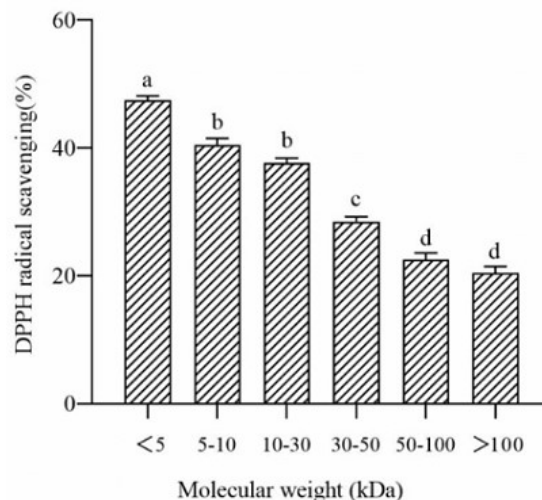


**Figure 4.** DPPH free radical scavenging ability of fractions from *Enteromorpha prolifera* with different molecular weights at 5 mg/mL. Values are expressed as mean  $\pm$  SD, n = 6. a,b,c,... means each parameter with different letters is significantly different at  $p < 0.05$ .

ultrafiltration system, the tyrosinase inhibition rate significantly ascended with the reduction in molecular weight from  $8.2 \pm 1.3\%$  (MW > 100 kDa) to  $52.4 \pm 3.6\%$  (MW < 5 kDa) (Wang et al., 2021). Zhou et al. (2021) reported that the inhibition rates of the hydrolysate obtained with 3 h hydrolysis from EP on monophenolase and diphenolase activity of mushroom tyrosinase were measured as 32.7% and 39.1%, respectively, while those values for crude EP were 16.3% and 21.1%. While those values for EP were 16.3% and 21.1%, respectively (Zhou et al., 2021). Our results were consistent with this study, i.e., the lower the molecular weight, the better the tyrosinase inhibitory activity.

### 3.4 Effect of molecular weight on DPPH radical scavenging activity

At a concentration of 5 mg/mL, different components of EPF showed varied Diphenyl-picrylhydrazyl (DPPH) scavenging capacity, as shown in Figure 4. With the decrease in molecular weight, the DPPH scavenging capacity was increased and reached 48.15% for EPF5. According to Zhou and Chen's research, the lower the molecular weight, the better the DPPH free radical scavenging ability. Zhou et al. (2021) found that the in vitro antioxidant activity of pectinase and glucoamylase degraded polysaccharides was significantly higher than that of EP (Zhou et al., 2021). The study by Chen et al. (2019) also showed that the DPPH free radical scavenging ability was gradually increased with a decrease in the molecular weight of fucoidan at the same concentration (Chen et al., 2019). Wang et al. (2022) reported that after hot water extraction, ethanol precipitation, and deproteinization by Sevage method, the *Benincasa hispida* polysaccharide showed preferable scavenging ability against DPPH free radicals and the higher the dose, the better the scavenging effect (Wang et al., 2022).

### 3.5 Effects of EPF5 on the melanogenesis and tyrosinase activity of B16 cells

B16 cells were treated with 10, 5, 2.5, 1, and 0.5 mg/mL of EP3, EPF5, and arbutin (Figure 5A). Results showed that with the increase in the concentration of samples, the cell viability decreased. Arbutin at > 1 mg/mL concentration showed significant cytotoxicity by inhibiting cell viability. However, EPF5 showed very limited cytotoxicity and EP3 showed no cytotoxicity compared to arbutin ( $p < 0.05$ ).

As shown in Figure 5B, five concentration gradients (25, 50, 100, 250, and 500  $\mu$ g/mL) for each sample were selected. With the increase in sample concentration, the inhibition rate of melanin synthesis increased. At 500  $\mu$ g/mL concentration, the inhibitory effect was highest of EPF5 at 44.36%. The inhibitory activity of EP3 on melanin synthesis by B16 cells was the lowest at 31.89%. In addition, the inhibitory activity of EPF5 was better than arbutin. Overall, EPF5 had superior inhibitory activity on melanogenesis.

As shown in Figure 5C, EP3, and EPF5 showed significantly different tyrosinase inhibitory activities. The inhibitory effect of EPF5 was superior to EP3 at the same concentration. At 500  $\mu$ g/mL concentration, the inhibitory activity of EP3 was 27.74% in comparison to 49.67% of EPF5. Similar to melanin synthesis inhibitory activity results, EPF5 showed significantly higher tyrosinase inhibitory activity than arbutin at concentrations of 50-250  $\mu$ g/mL.

According to Chen et al. (2019) fucoidan with different molecular weight within 20 mg/mL caused no cytotoxicity in mouse B16 cells and the comparable melanin inhibition ability with arbutin was observed, although none of the fucoidan fractions was more active than arbutin at the same concentration in the tested range (Chen et al., 2019). A study of melanogenesis

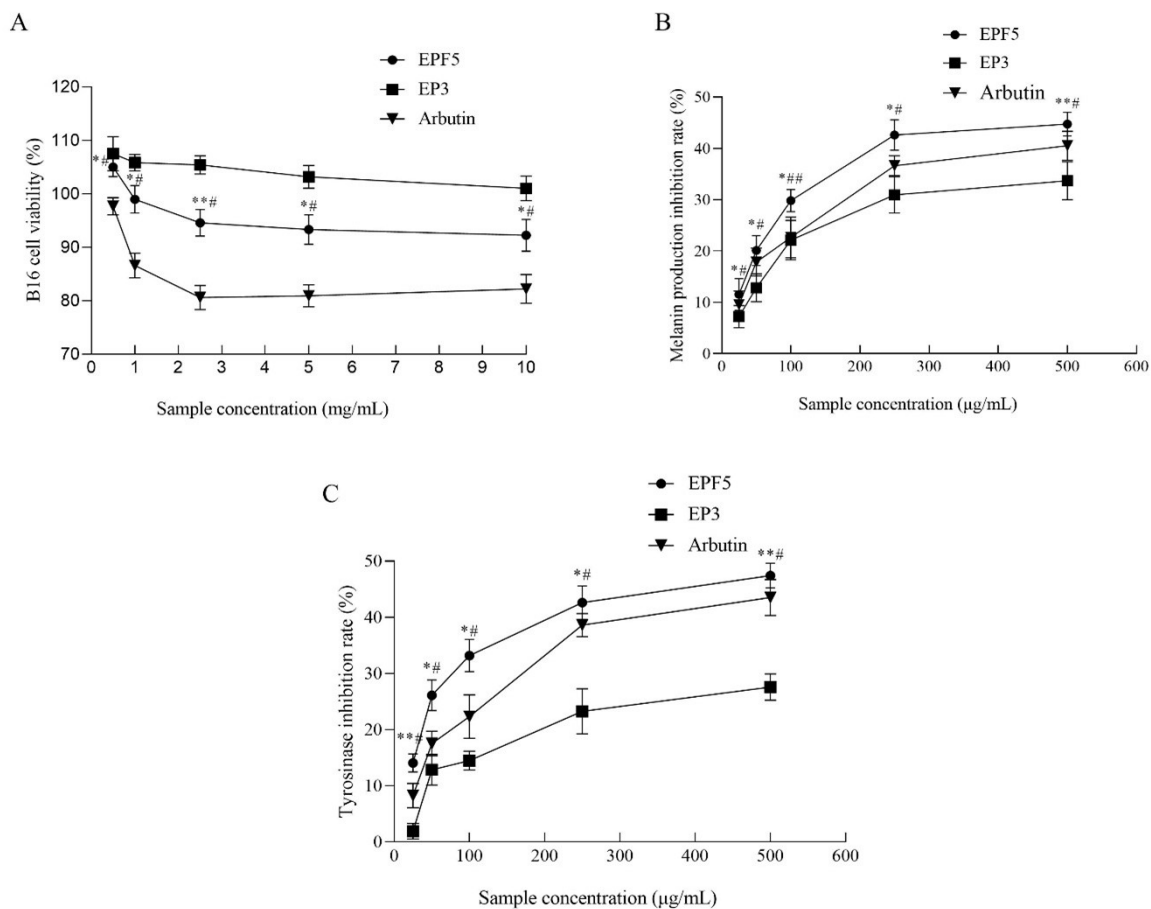


**Figure 5.** Effect of *Enteromorpha prolifera* polysaccharides (EP3) and polysaccharide fraction with MW < 5 kDa (EPF5) on the cell viability (A), melanogenesis (B), and tyrosinase activity (C) of B16 cells. Data are presented as mean  $\pm$  SD, n = 10. Tukey-Kramer HSD test was used for statistical analysis. \* $p < 0.05$  and \*\* $p < 0.01$  versus the Arbutin group; # $p < 0.05$  and ## $p < 0.01$  versus the EP group.

inhibitory activity of low MW fucoidan showed that the melanin content of B16 melanoma cells is reduced by about 50% in the samples treated with 6 kDa fucoidan at the dose of 10 mg/mL (Park & Choi, 2017). Choi et al. (2014) also reported that the melanin content in melanoma cells reduces with a decrease in laminarin MW (Choi et al., 2014). Sulfated galactans isolated from red alga showed no significant effect on cell viability, and a significant decrease in melanin levels in cells in a dose-dependent manner (Pratoomthai et al., 2018). Red ginseng polysaccharides prepared by ethanol fractionation also showed no cytotoxicity (Kim et al., 2022). Our findings confirmed that EP inhibited melanin synthesis activity in B16 cells, and that the lower the molecular weight (within a certain range), the better the tyrosinase inhibitory activity. EPF5 has greater effects and lower toxicity than arbutin, which has limited application due to cytotoxicity.

### 3.6 Effect of EPF5 on reactive oxygen species content in B16 cells

The production and increase of reactive oxygen species (ROS) is the beginning of oxidative damage, and can cause damage to

macromolecular substances in organisms, induce various diseases, accelerate the aging of body, and thus seriously affect human health (Li et al., 2022; Liu & Li, 2021). The ROS content in cells can be measured based on the green fluorescence intensity of ROS. As shown in Figure 6A, the green fluorescence intensity of the blank group was high (2243.40), which indicated that UVB radiation produced a large amount of ROS in B16 cells (Liu et al., 2016). After the addition of arbutin, EP3, and EPF5, the fluorescence intensity of ROS in cells was significantly reduced ( $p < 0.05$ ) by 50.47%, 55.41%, and 80.56%, respectively. These results indicated that EPF5 could significantly eliminate ROS produced in B16 cells and effectively protect the intracellular antioxidant system.

### 3.7 Kinetic inhibition of tyrosinase activity by EPF

The enzyme kinetics in the presence of fucoidan were investigated using double-reciprocal Lineweaver-Burk plots. The changes in both the apparent  $V_{max}$  and  $K_m$  values were observed, indicating that EPF5 induced a mixed type of inhibition (Figure 7A). This finding is consistent with the findings of Zhou et al. (2021). Therefore, EPF5 is bound to both the free

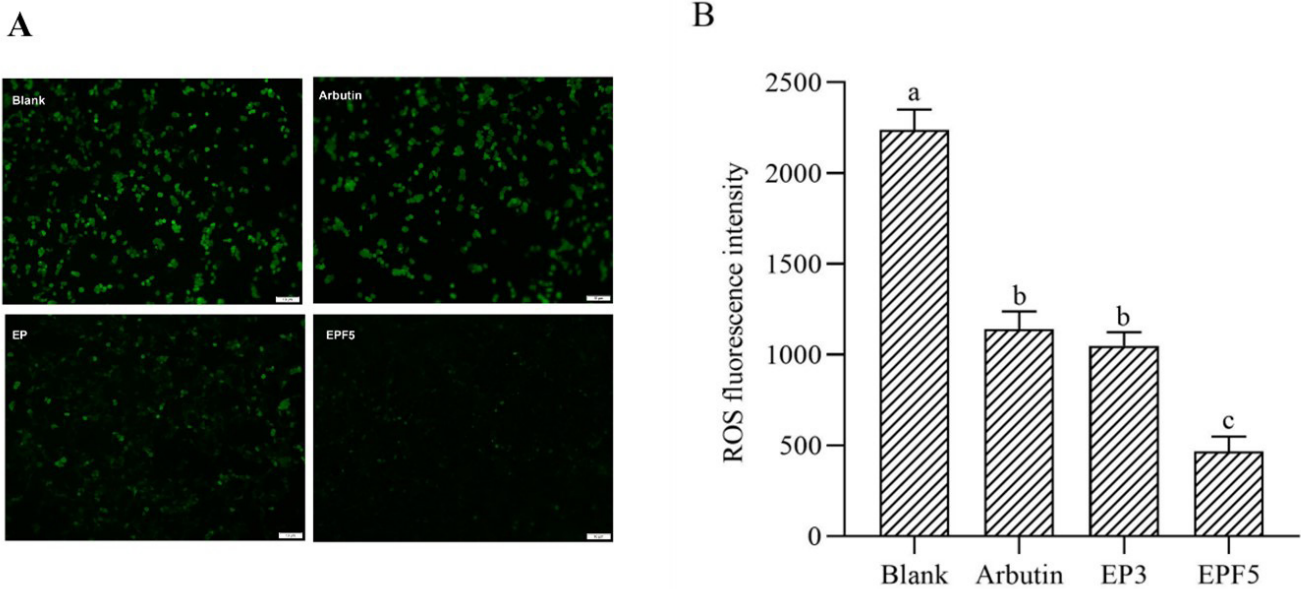


**Figure 6.** B16 cells treated with distilled water, arbutin, *Enteromorpha prolifera* polysaccharides (EP3), and polysaccharide fraction with MW < 5 kDa (EPF5) under a fluorescence microscope (A), and ROS content in B16 cells treated with distilled water, arbutin, EP3, and EPF5 (B).

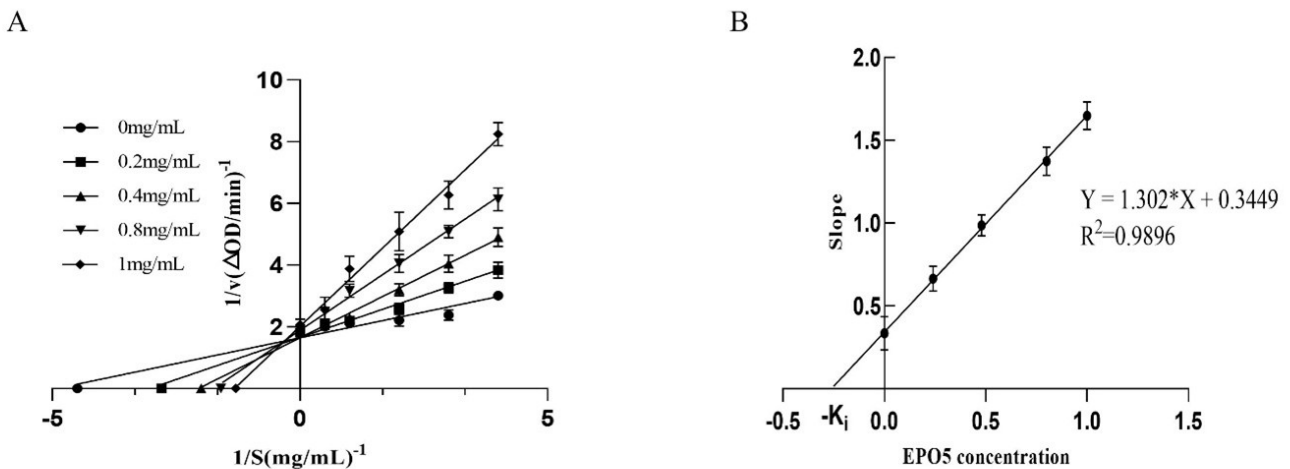


**Figure 7.** Kinetic analysis of tyrosinase inhibition and the antibrowning effect of *Enteromorpha prolifera* polysaccharide with MW < 5 kDa (EPF5). Double-reciprocal Lineweaver-Burk plots of the tyrosinase inhibitory effect of EPF5 (A), replot of the slope data from A versus the concentration of EPF5 (B). Values are expressed as mean  $\pm$  SD, n = 3.

enzyme and the enzyme-substrate complex. The inhibition reaction was reversible, and the biphasic inactivation process reflected the stable structure of tyrosinase by implying the accumulation of intermediates accompanying thermodynamic changes during inactivation (Wang et al., 2012). It is possible that EPF5 can form hydrogen bonds with tyrosinase and interact with enzyme-substrate complexes via hydrogen bonds, resulting in a conformational change of tyrosinase and inhibition of substrate entry into the active site of the enzyme, while also inhibiting

product generation from the resulting EPF5-enzyme-substrate complex (Zhou et al., 2021).

It is well known that inhibitors with lower inhibitor constant ( $K_i$ ) values bind more tightly to the enzyme suggesting their high inhibition efficiency (Sari et al., 2019). As shown in Figure 7B, the slope data from Figure 7A showed a linear fit to EPF5 concentration with a  $K_i$  of  $0.254 \pm 0.067$  mg/mL, similar to the  $K_i$  (0.236 mg/mL) reported by Yu & Sun (2014) and lower than the  $K_i$  ( $0.792 \pm 0.183$  mg/mL) reported by Wang et al.

(2012). The results indicated that EPF5 was an effective tyrosinase inhibitor.

## 4 Conclusion

In summary, EP3 purified from crude EP with the highest polysaccharide content and the best tyrosinase inhibition rate was used for the following degradation. Enzymatic hydrolysis had the best degradation effect in terms of tyrosinase inhibition rate. The enzymatic hydrolysate fraction with molecular weight below 5 kDa (EPF5) showed the best tyrosinase- and melanogenesis-inhibitory and antioxidant activities through *in vitro* and cell experiments and without apparent cytotoxicity. The kinetic analysis of tyrosinase inhibition suggested that EPF5 might inhibit tyrosinase through competitive-uncompetitive mixed-type way. Based on these findings, it can be speculated that EPF5 from *Enteromorpha prolifera* could be used as a safe and effective ingredient in skin-whitening cosmetics and also as an antibrowning agent in food and agriculture industries.

## Acknowledgements

The research was supported by basic research funds for the universities of Zhejiang, Zhejiang Institute of Economics and Trade (20SBYB06).

## References

- Arokiarajan, M. S., Thirunavukkarasu, R., Joseph, J., Ekaterina, O., & Aruni, W. (2022). Advance research in biomedical applications on marine sulfated polysaccharide. *International Journal of Biological Macromolecules*, 194, 870-881. <http://dx.doi.org/10.1016/j.ijbiomac.2021.11.142>. PMID:34843816.
- Cao, Q., Zhao, J. R., Xing, M. C., Xiao, H., Zhang, Q., Liang, H., Ji, A. G., & Song, S. L. (2020). Current research landscape of marine-derived anti-atherosclerotic substances. *Marine Drugs*, 18(9), 440. <http://dx.doi.org/10.3390/md18090440>. PMID:32854344.
- Chen, B. J., Shi, M. J., Cui, S., Hao, S. X., Hider, R. C., & Zhou, T. (2016). Improved antioxidant and anti-tyrosinase activity of polysaccharide from *Sargassum fusiforme* by degradation. *International Journal of Biological Macromolecules*, 92, 715-722. <http://dx.doi.org/10.1016/j.ijbiomac.2016.07.082>. PMID:27471085.
- Chen, Q., Kou, L., Wang, F., & Wang, Y. (2019). Size-dependent whitening activity of enzyme-degraded fucoidan from *Laminaria japonica*. *Carbohydrate Polymers*, 225, 115211. <http://dx.doi.org/10.1016/j.carbpol.2019.115211>. PMID:31521267.
- Choi, J.-i., Lee, S. G., Han, S. J., Cho, M., & Lee, P. C. (2014). Effect of gamma irradiation on the structure of fucoidan. *Radiation Physics and Chemistry*, 100, 54-58. <http://dx.doi.org/10.1016/j.radphyschem.2014.03.018>.
- Fernando, I. P. S., Kim, K.-N., Kim, D., & Jeon, Y.-J. (2019). Algal polysaccharides: potential bioactive substances for cosmeceutical applications. *Critical Reviews in Biotechnology*, 39(1), 99-113. <http://dx.doi.org/10.1080/07388551.2018.1503995>. PMID:30198346.
- Goenka, S., & Simon, S. R. (2021). Depigmenting effect of Xanthohumol from hop extract in MNT-1 human melanoma cells and normal human melanocytes. *Biochemistry and Biophysics Reports*, 26, 100955. <http://dx.doi.org/10.1016/j.bbrep.2021.100955>. PMID:33681480.
- Gu, X., Fu, L., Pan, A., Gui, Y., Zhang, Q., & Li, J. (2021). Multifunctional alkalophilic  $\alpha$ -amylase with diverse raw seaweed degrading activities. *AMB Express*, 11(1), 139. <http://dx.doi.org/10.1186/s13568-021-01300-x>. PMID:34669086.
- Guo, H., Zhang, W., Jiang, Y., Wang, H., Chen, G., & Guo, M. (2019). Physicochemical, structural, and biological properties of polysaccharides from dandelion. *Molecules*, 24(8), 1485. <http://dx.doi.org/10.3390/molecules24081485>. PMID:30991766.
- Kim, H., Cho, S. M., Kim, G. W., Hong, K. B., Suh, H. G., & Yu, K. W. (2022). Red ginseng polysaccharide alleviates cytotoxicity and promotes anti-inflammatory activity of ginsenosides. *Food Science and Technology*, 42, e52220. <http://dx.doi.org/10.1590/fst.52220>.
- Li, Q., Qin, X. K., Yu, Y., Quan, S. J., & Xiao, P. (2022). *Schisandra chinensis* polysaccharides exerts anti-oxidative effect in vitro through Keap1-Nrf2-ARE pathway. *Food Science and Technology*, 42, e44621. <http://dx.doi.org/10.1590/fst.44621>.
- Liu, M. H., Zhang, Y., He, J., Tan, T. P., Wu, S. J., Guo, D. M., He, H., Peng, J., Tang, Z. H., & Jiang, Z. S. (2016). Hydrogen sulfide protects H9c2 cardiac cells against doxorubicin-induced cytotoxicity through the PI3K/Akt/FoxO3a pathway. *International Journal of Molecular Medicine*, 37(6), 1661-1668. <http://dx.doi.org/10.3892/ijmm.2016.2563>. PMID:27081862.
- Liu, Y., & Li, S. M. (2021). Extraction optimization and antioxidant activity of *Phyllanthus urinaria* polysaccharides. *Food Science and Technology*, 41(Suppl. 1), 91-97. <http://dx.doi.org/10.1590/fst.11320>.
- Liu, Y., Wu, X., Jin, W., & Guo, Y. (2020). Immunomodulatory effects of a low-molecular weight polysaccharide from *Enteromorpha prolifera* on RAW 264.7 macrophages and cyclophosphamide-induced immunosuppression mouse models. *Marine Drugs*, 18(7), 340. <http://dx.doi.org/10.3390/md18070340>. PMID:32605327.
- Molina, A. K., Vega, E. N., Pereira, C., Dias, M. I., Heleno, S. A., Rodrigues, P., Fernandes, I. P., Barreiro, M. F., Kostić, M., Soković, M., Barreira, J. C. M., Barros, L., & Ferreira, I. C. F. R. (2019). Promising antioxidant and antimicrobial food colourants from *Lonicera caerulea* L. var. *Kamtschatica*. *Antioxidants*, 8(9), 394. <http://dx.doi.org/10.3390/antiox8090394>. PMID:31547323.
- Ning, L., Yao, Z., & Zhu, B. (2022). Ulva (*Enteromorpha*) polysaccharides and oligosaccharides: a potential functional food source from green-tide-forming macroalgae. *Marine Drugs*, 20(3), 202. <http://dx.doi.org/10.3390/md20030202>. PMID:35323501.
- Ou, J. M., Yu, Z. Y., Qiu, M. K., Dai, Y. X., Dong, Q., Shen, J., Wang, X. F., Liu, Y. B., Quan, Z. W., & Fei, Z. W. (2014). Knockdown of VEGFR2 inhibits proliferation and induces apoptosis in hemangioma-derived endothelial cells. *European Journal of Histochemistry*, 58(1), 2263. <http://dx.doi.org/10.4081/ejh.2014.2263>. PMID:24704994.
- Park, E. J., & Choi, J. I. (2017). Melanogenesis inhibitory effect of low molecular weight fucoidan from *Undaria pinnatifida*. *Journal of Applied Phycology*, 29(5), 2213-2217. <http://dx.doi.org/10.1007/s10811-016-1048-4>.
- Peng, Z., Li, Y., Tan, L., Chen, L., Shi, Q., Zeng, Q.-H., Liu, H., Wang, J. J., & Zhao, Y. (2022). Anti-tyrosinase, antioxidant and antibacterial activities of gallic acid-benzylidenehydrazine hybrids and their application in preservation of fresh-cut apples and shrimps. *Food Chemistry*, 378, 132127. <http://dx.doi.org/10.1016/j.foodchem.2022.132127>. PMID:35033723.
- Pratoomthai, B., Songtavisin, T., Gangnonngiw, W., & Wongprasert, K. (2018). In vitro inhibitory effect of sulfated galactans isolated from red alga *Gracilaria fisheri* on melanogenesis in B16F10 melanoma cells. *Journal of Applied Phycology*, 30(4), 2611-2618. <http://dx.doi.org/10.1007/s10811-018-1469-3>.
- Sari, S., Barut, B., Özel, A., & Şöhretoğlu, D. (2019). Tyrosinase inhibitory effects of *Vinca major* and its secondary metabolites: enzyme kinetics and in silico inhibition model of the metabolites validated

- by pharmacophore modelling. *Bioorganic Chemistry*, 92, 103259. <http://dx.doi.org/10.1016/j.bioorg.2019.103259>. PMID:31518762.
- Wang, K. W., Sheng, X. Y., Chen, X. J., Zhu, X. Y., & Yang, C. (2022). Characterization and antioxidant activities of polysaccharide extracted from *Benincasa hispida* var. *chieh-qua* How. *Food Science and Technology*, 42, e88421. <http://dx.doi.org/10.1590/fst.88421>.
- Wang, L., Oh, J. Y., Jayawardena, T. U., Jeon, Y. J., & Ryu, B. (2020). Anti-inflammatory and anti-melanogenesis activities of sulfated polysaccharides isolated from *Hizikia fusiforme*: short communication. *International Journal of Biological Macromolecules*, 142, 545-550. <http://dx.doi.org/10.1016/j.ijbiomac.2019.09.128>. PMID:31715243.
- Wang, Y., Niu, D. J., Que, F., Li, Y., & Chen, Q. R. (2021). Low molecular weight fucoidan prepared by fucoidanase degradation-a promising browning inhibitor. *Lebensmittel-Wissenschaft + Technologie*, 148, 111739. <http://dx.doi.org/10.1016/j.lwt.2021.111739>.
- Wang, Z.-J., Si, Y.-X., Oh, S., Yang, J.-M., Yin, S.-J., Park, Y.-D., Lee, J., & Qian, G.-Y. (2012). The effect of fucoidan on tyrosinase: computational molecular dynamics integrating inhibition kinetics. *Journal of Biomolecular Structure & Dynamics*, 30(4), 460-473. <http://dx.doi.org/10.1080/07391102.2012.682211>. PMID:22694253.
- Wassie, T., Niu, K., Xie, C., Wang, H., & Xin, W. (2021). Extraction techniques, biological activities and health benefits of marine algae *Enteromorpha prolifera* polysaccharide. *Frontiers in Nutrition*, 8, 747928. <http://dx.doi.org/10.3389/fnut.2021.747928>. PMID:34692752.
- Xia, Z., Yuan, H., Liu, J., Sun, Y., Tong, Y., Zhao, S., Xia, J., Li, S., Hu, M., Cao, J., Zhang, J., & He, P. (2022). A review of physical, chemical, and biological green tide prevention methods in the Southern Yellow Sea. *Marine Pollution Bulletin*, 180, 113772. <http://dx.doi.org/10.1016/j.marpolbul.2022.113772>. PMID:35623218.
- Yin, Z., Zhang, W., Zhang, J., Liu, H., Guo, Q., Chen, L., Wang, J., & Kang, W. (2019). Two novel polysaccharides in *psoralea corylifolia* L and anti-A549 lung cancer cells activity in vitro. *Molecules*, 24(20), 3733. <http://dx.doi.org/10.3390/molecules24203733>. PMID:31623207.
- Yu, P., & Sun, H. (2014). Purification of a fucoidan from kelp polysaccharide and its inhibitory kinetics for tyrosinase. *Carbohydrate Polymers*, 99, 278-283. <http://dx.doi.org/10.1016/j.carbpol.2013.08.033>. PMID:24274507.
- Zhang, X. W., Bian, G. L., Kang, P. Y., Cheng, X. J., Yan, K., Liu, Y. L., Gao, Y. X., & Li, D. Q. (2021). Recent advance in the discovery of tyrosinase inhibitors from natural sources via separation methods. *Journal of Enzyme Inhibition and Medicinal Chemistry*, 36(1), 2104-2117. <http://dx.doi.org/10.1080/14756366.2021.1983559>. PMID:34579614.
- Zhong, K., Zhang, Q., Tong, L. T., Liu, L. Y., Zhou, X. R., & Zhou, S. M. (2015). Molecular weight degradation and rheological properties of schizophyllan under ultrasonic treatment. *Ultrasonics Sonochemistry*, 23, 75-80. <http://dx.doi.org/10.1016/j.ultsonch.2014.09.008>. PMID:25263766.
- Zhou, J. M., Shi, M. J., Wei, X. Y., & Zhou, T. (2021). Enzymatic degradation of polysaccharide from *Enteromorpha prolifera*: an efficient way to enhance its antioxidant and tyrosinase inhibitory activities. *Journal of Food Measurement and Characterization*, 15(5), 4623-4634. <http://dx.doi.org/10.1007/s11694-021-01039-w>.
- Zhu, Y. Z., Chen, K., Chen, Y. L., Zhang, C. J., Xie, Y. Y., Hider, R. C., & Zhou, T. (2022). Design and synthesis of novel stilbene-hydroxypyridinone hybrids as tyrosinase inhibitors and their application in the anti-browning of freshly-cut apples. *Food Chemistry*, 385, 132730. <http://dx.doi.org/10.1016/j.foodchem.2022.132730>. PMID:35318180.